3D-Printed HASEL Actuators With Integrated Fluidic Piezoresistive Pressure Sensor for Cardiac Assist Applications*

Evan Zhang
The Harker School
San Jose, USA
evan.r.zhang@gmail.com

Alex Chortos*
School of Mechanical Engineering
Purdue University
West Lafayette, USA
achortos@purdue.edu
*Corresponding author

***Abstract*—This work presents a fully 3D printed Hydraulically Amplified Self-Healing Electrostatic (HASEL) actuator integrated with a soft piezoresistive force sensor for cardiac assist applications. The actuator is fabricated via direct ink write (DIW) 3D printing, enabling precise and personalizable construction of elastomer shells, soft electrodes, and liquid dielectric cavities. A fluidic piezoresistive sensor is integrated for monitoring of pressure output while preserving the actuator's compliant properties. The actuator achieves up to 87.9% strain with rapid response and repeatability up to 7.5 Hz. The sensor also demonstrates minimal hysteresis due to the fluidic reset mechanism, and it exhibits a clear correlation between applied force and resistance when coupled with the actuator. This self-sensing system enables closed-loop control through correlating voltage, resistance, and force and meets the performance requirements for mechanical support of the heart. Compared to existing VADs, this approach offers improved bio-compatibility, adaptability, and sensing. This work establishes a foundation for self-sensing soft robotic systems for future biomedical devices.**

***Index Terms*—HASEL actuators, cardiac assist, self-sensing**

I. Introduction

Cardiovascular diseases are the leading cause of death globally, claiming 17.9 million lives each year. Heart Failure (HF), one of the most serious variations of cardiovascular disease, is a chronic condition in which the heart is unable to pump enough blood to support the body's needs [1]. While simple lifestyle changes and medication can treat HF in its early stages, more serious cases, called class III or IV, often require more intensive treatment. For these scenarios, a heart transplant is the ideal treatment [2]. However, the demand for donor hearts far exceeds their supply, leaving many individuals without access to it [3]. These challenges underscore the urgent need for alternative solutions to address the growing issue of heart failure.

Mechanical support devices have been developed to aid the heart in its pumping function and treat patients with HF [4]. Ventricular Assist Devices (VADs), in particular, have evolved significantly in recent years. Modern VADs feature advanced designs in an attempt to minimize complications such as hemolysis and thrombosis [5] [6]. As a result, there is an increasing demand for innovative approaches to HF that prioritize effectiveness and safety.

Soft robotics has emerged as a promising solution for the limitations of VADs. Unlike rigid robots, soft robots are composed of flexible, deformable materials that enable them to operate in complex, delicate, and unpredictable environments [7]. By mimicking the actions of biological systems, soft robots are uniquely positioned to replicate the motion of muscles such as the heart. This makes soft actuators especially well suited for applications relating to human-machine interaction, such as with cardiac assist devices [8]. Hydraulically Amplified Self-Healing Electrostatic (HASEL) actuators combine liquid dielectrics with soft, elastomer shells and electrodes to create deformation and motion. These actuators provide high force, compliance, and reliability via self-healing, making them fit for healthcare robotics applications [8].

We propose a 3D-printed HASEL actuator integrated with a fluidic piezoresistive pressure sensor for use in cardiac assist applications. Our contributions include the integration of a fluidic piezoresistive pressure sensor into a 3D-printed HASEL actuator, the use of DIW 3D printing for customizable fabrication, and the demonstration of pressure-sensitive actuation. The actuator produces relevant strain while maintaining flexibility and biocompatibility required for the application. By leveraging direct ink write (DIW) 3D printing, we achieve precise fabrication of the elastomer shell, electrodes, and sensor in a customizable fabrication process. The integrated sensor provides feedback on pressure changes as a result of actuation. This study addresses key functional elements of soft ventricular assist devices, such as soft force sensing as well as rapid and repeatable actuation. This work serves as a foundation to explore soft, biocompatible alternatives to rigid VADs.

II. Related Works

Various types of soft actuators have been explored for use as cardiac assist devices. One area of progress is with pneumatic devices, which rely on air to produce an expanding motion.

This work was partially supported by NSF grant 2301509.

However, their reliance on external compressor systems and pneumatic drivelines limits their portability and adaptability and leads to infections [9] [10] [11]. A demonstration with shape memory alloys [12] shows that artificial muscles can have lower energy consumption than VADs, but with the critical limitation that they operate at unsafe temperatures of 70 ºC. Magnetically responsive actuators allow straightforward control by adjusting the magnetic field's direction and magnitude, but suffer from high power consumption and limited field penetration [13].

Electronically driven actuators have garnered significant attention for their precise controllability, rapid response times, and compatibility with modern energy systems, forming a strong foundation for next-generation cardiac assist devices [14]. Among these, dielectric elastomer actuators (DEAs) have demonstrated significant potential. DEAs achieve actuation through Coulombic attraction between two soft electrodes and a flexible membrane [15] [16]. They exhibit precise actuation and quick responses but are limited by dielectric breakdown, compromising long-term reliability. To overcome this, HASEL actuators have been developed [17].

While traditional DEAs fail upon breakdown, HASEL actuators use a liquid dielectric that can flow back and repair damaged areas [17]. This allows consistent performance and minimal energy loss even after multiple breakdowns. Prior studies show that HASEL actuators can deliver sufficient force with just one layer, whereas DEAs may require several [18]. HASEL actuators offer both linear contraction and out-of-plane expansion, increasing their versatility and effectiveness for cardiac assist applications.

Previous research has demonstrated the effectiveness of HASEL actuators. For example, Pirozzi et al. developed a HASEL-based device designed to wrap around the pulmonary artery to assist the function of the right ventricle [18]. However, the actuator is fabricated using inextensible thin films, which are vulnerable to fatigue cracking and degradation. The system also achieves a maximum strain of 5%, which may be insufficient for cases where a larger change is needed. Fabrication is also through manual means, increasing the risk of defects. Finally, the integrated pressure sensor features a rigid structure, creating a mismatch with the soft structure of the actuator and making it inflexible for compliance around complex organs.

Integrating HASELs with soft pressure sensors is also critical in biomedical and robotic systems because they enable real-time feedback and adaptive control. Previous studies regarding self-sensing HASEL actuators have investigated displacement control and sensing using capacitive [19] and magnetic [20] approaches. Previous HASEL actuators have integrated rigid force sensors [18], but these rigid sensors introduce mechanical mismatch, reducing the overall compliance and conformability of the system. As a result, they are poorly suited for long-term integration in soft robotic or implantable biomedical applications. There have been limited reports regarding integrated force sensing for HASELs using soft components. To this extent, we propose a fully 3D-printed HASEL actuator integrated with a fluidic piezoresistive pressure sensor for use in cardiac assist applications.

III. Methodology

A. Actuator Design and 3D Printing Process

Given the highly integrated nature of soft machines, additive manufacturing is an appealing method to fabricate them as it allows for rapid tailoring of dimensions and device or material properties. Direct ink write (DIW) printers have been used to print the desired chambers and indents present in previous pneumatic-driven actuators, as well as other electrostatic actuators. It is also a contactless process that can control the thickness of the deposited layers as well as vary them during one layer it prints. This creates detailed features even on fragile and thin substrates. These processes enable straightforward customization of the final device without revamping all auxiliary elements like molds. It also increases the reproducibility of final structures as it ensures uniformity on all surfaces.

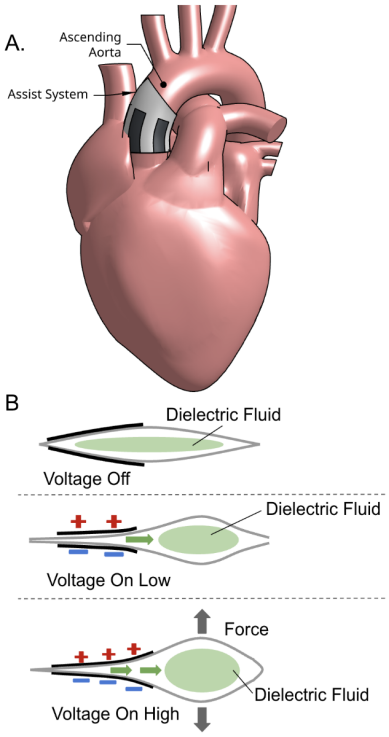

Fig. 1. (A) Placement of HASEL on the ascending aorta of the heart and left ventricle to aid in pumping of oxygenated blood to the body. (B) Operating principle of standard HASEL Actuator.

The design of a HASEL actuator is shown in Fig.1B, and the fabrication process is shown in Fig.2A and Fig.2B. Individual actuators are shown in Figure 2B, and multiple actuators are interconnected to wrap around the ascending aorta of the heart (Fig.1A), aiding the left ventricle in supplying oxygenated blood to the body or around the pulmonary artery, aiding the right ventricle. These actuators consist of three components - an elastomer shell, soft electrodes, and a liquid dielectric.

The operating principle of HASELS, as shown in Fig.1B is such that when a voltage is applied across the electrodes,

electrostatic forces compress the liquid dielectric and displace it, deforming the elastomer membrane and producing force. These actuators consist of three components - an elastomer shell, soft electrodes, and a liquid dielectric. First, soft, conductive electrodes are printed. EcoFlex 00-50 (Smooth-on) is mixed with carbon black (Acetylated carbon black from Fisher, AA3972430) at 16 parts per hundred rubber (PHR). After speed mixing, the composition is roll milled three times to allow the carbon black to disperse evenly and prevent aggregation. The electrodes are printed onto a glass slide at a thickness of $410\mu m$.

For the elastomer dielectric, EcoFlex 00-50 is chosen for its flexibility and biocompatibility [21]. To create the elastomer shell, Part A and Part B of EcoFlex 00-50 are combined at a 1:1 ratio. To increase the viscosity of the ink for 3D printing, M5 Silica is added to the silicone at a ratio of 10 grams of silicone to 0.4 grams of silica. Slo-Jo retarder is added to the ink at a ratio of 10 g to 0.08g to increase the pot life of the elastomer inside the extruder. When printed, this gives a membrane which is 0.8 mm thick with a 0.5 mm deep indented region for the liquid dielectric. The elastomer dielectric is printed with a lateral area of 55 mm by 35 mm, and the indented region has dimensions of 30 mm by 20 mm. After they are printed, the electrode and membrane are fully cured. The use of 3D printing allows the size of both the electrodes and the dielectric to be easily altered.

A dissolvable ink is used as a temporary support to maintain the shape of internal cavities until the rest of the structure is fully fabricated. It is made from Polyethylene glycol (PEG) mixed with M5 fumed silica at a ratio of 10:1. This ink is printed to fill the cavity entirely. These fabrication steps are performed twice per actuator in order to produce two cured membrane–electrode structures, which are later bonded together to form a complete sealed pouch.

To seal the pouch, a layer of ink with the same composition as the membrane is printed on the raised edges of the membrane. A second membrane is placed inverted on top of the adhesive, and all edges are aligned. The adhesive is cured to form a sealed pouch. To remove the sacrificial supports, ethanol is injected into the cavity, dissolving them. FR3 dielectric fluid is inserted into the cavity, and any openings are sealed using EcoFlex 00-50. The final geometry of the actuator is shown in Figure 2B.

B. Sensor Fabrication and Integration

A piezoresistive pressure sensor is integrated in the actuator to monitor its force output. It consists of two electrodes placed vertically above each other. When a force is applied on the pressure sensor, the contact area between the two electrodes varies. Under larger forces, the area increases, thus decreasing the electrical resistance between the two electrodes. Values of electrical resistance can be correlated with force.

The two electrodes are made stretchable using the same formulation present in the actuator's electrodes. They are separated with an insulating layer of EcoFlex 00-50 around the borders, and the area in the center of the electrodes is left

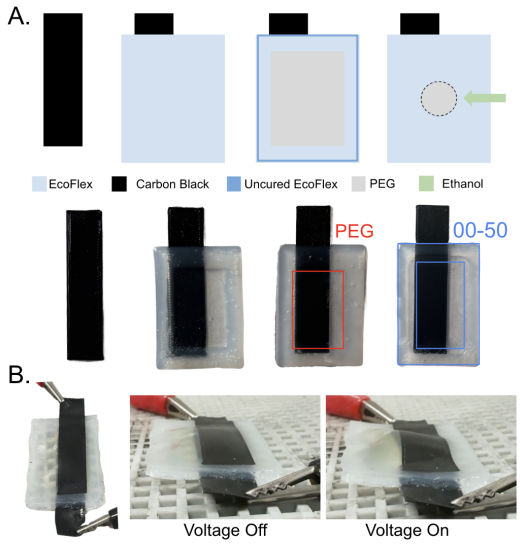

Fig. 2. (A) Layer by layer order of 3D printing (B) Complete HASEL and demonstration of deformation.

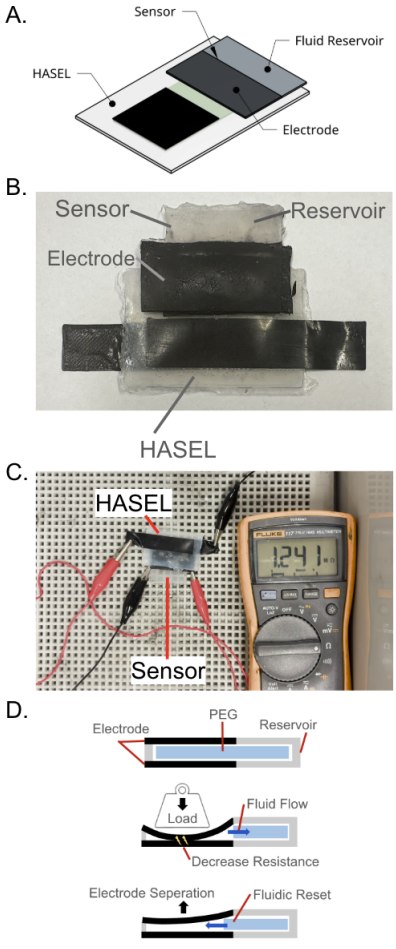

Fig. 3. (A): Diagram of placement of sensor on HASEL actuator. (B) Integration of HASEL and force sensor. (C) Experimental setup for resistance measurements.

open to allow them to make contact. However, the electrodes, when pressed together, have a tendency to adhere to one another. This occurs because the silicone is naturally tacky, and surface energy is sufficient to cause the thin electrodes to stick together. As a result, the sensor may not fully reset after activation.

To overcome this, fluids are used to expedite the mechanical reset, similar in principle to the dielectric fluid's role in resetting HASEL actuators. When the electrodes are printed, a section to the side is also printed using EcoFlex 00-50. This creates a reservoir where fluid can flow to when the sensor is under load, and where fluid can leave when the load is removed. The fluid acts as a temporary physical barrier that resists complete adhesion between the electrode surfaces, helping to separate them after unloading. During compression, the fluid is displaced from the sensing region into the adjacent reservoir, minimizing adhesion and facilitating electrode separation. Once the compressive force is removed, the elastomer's elasticity drives the fluid back into the sensing region, providing force for restoring the electrodes to their original uncompressed state. This final geometry of the sensor is shown in Fig.3B.

The fluid selected to fill the reservoir is polyethylene glycol (PEG) to avoid soaking into the electrode and accelerating its degradation. Because of its polarity, PEG does not enter the hydrophobic silicone. This reduces swelling in the electrodes, which could compromise and degrade the electrodes, changing the sensor's characteristics over time or potentially leading to failure.

The sensor is placed on the actuation area of the HASEL, with the main sensing portion directly over the areas of the HASEL with the largest deformation, as in Fig.3B, and the reservoir positioned away from the electrodes to minimize its impact on the HASEL's actuation. EcoFlex 00-50 is printed onto the sensor and used as adhesive.

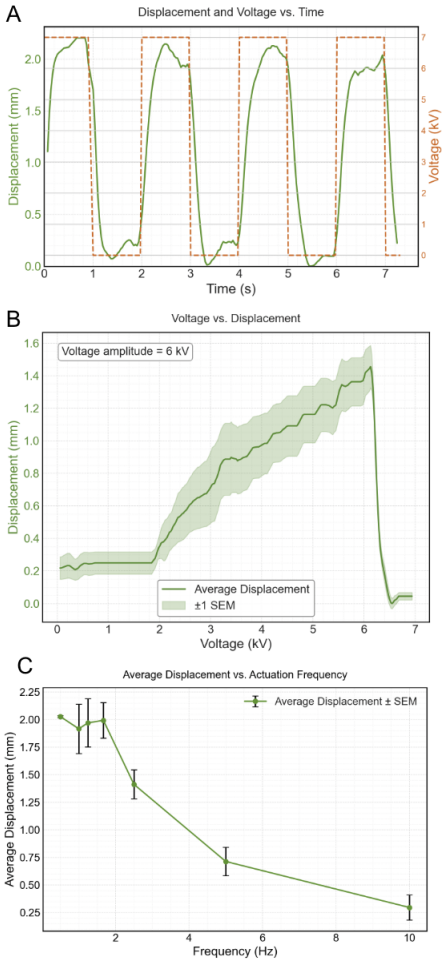

Fig. 4. (A) Deformation of the actuator as a function of time. Voltage input is a 7 kV square waveform with a period of 2 seconds. (B) Displacement of HASEL as voltage ramps from 0 to 6 kV. (C) Displacement of HASEL as a function of frequency of actuation.

IV. Results and Discussion

A. Actuator Characterization

To evaluate the viability of the 3D-printed HASEL, we characterize its displacement under various voltage inputs. These experiments aim to assess the device's ability to generate the necessary deformation for effective mechanical stimulation of the heart.

The displacement as a function of time is shown in Fig.4A. The actuator demonstrates a rapid actuation response, with the device achieving both the maximum deformation after voltage is applied and returning to its original position after voltage is removed within one second. The most rapid deformation response is within the first 0.4 seconds, stabilizing afterwards. The average maximum displacement in an actuation cycle is 2.11 mm, meaning the average strain reached is 87.9%, exceeding the necessary 20% outlined by the design criteria. The actuator is shown to consistently return to its initial configuration as a result of the elasticity of the EcoFlex membrane shell. There was no permanent deformation observed across multiple actuation cycles, indicating repeatability and mechanical durability. This is essential for patient safety in cardiac applications, where there is continuous cyclic loading at a high frequency.

The relationship between applied voltage and actuator displacement is nearly linear in Fig.4B, most notably between three and six volts as voltage increments. A linear relationship between voltage and displacement in a HASEL actuator is better for control because it makes the system more predictable and easier to manage. It allows for simpler control algorithms (like PID), improves accuracy, and reduces the need for complex compensation, making real-time control more reliable and efficient. The minimum activation voltage is 2 kV, and at 6 kV, the actuator achieves an average of 1.45 mm displacement, or a strain of 60.4

The ability to tune the displacement is critical for clinical use, as it enables precise control over the magnitude of assistance. During systole, for example, greater compression is required, while less compression is preferred during diastole or the resting state. Because the actuator can reach high strain values, and because the relationship between strain and voltage

is linear, the actuator's performance can be adapted to the needs of individual patients, who may require slightly different treatments.

Tests across different frequencies range from 0.25 Hz to 10 Hz, as shown in Fig.4C. The actuator consistently reaches maximum displacement from 0.25 to 2 Hz. After 2 Hz, the actuator's displacement begins to drop. The minimum displacement for 20% strain is 0.48 mm, which is shown to be at 7.5 Hz. This reduction in displacement can be attributed to insufficient time for the fluid to fully redistribute across the actuator. Given that the human heart beats at 1-2 Hz, this performance suggests that the actuator is well-suited for such pacing. It maintains the ability to reach maximum displacement up until 2 Hz, and can remain above 20% displacement until 7.5 Hz. Further optimization of fluid viscosity and stiffness could extend applications to higher-frequency situations as well.

To simulate realistic loading conditions, an 8g mass is applied to the actuator during operation. Displacement is tracked over time to assess the deformation changes under load. The device consistently lifted the load and maintained an average peak displacement of 2.08 mm. Furthermore, the addition of a load improved the stability of the displacement near the top of the actuation cycle, as shown in Fig5. In unloaded trials, this volatility likely stems from the inertia of the liquid flowing as well as the membrane's elasticity. With a load present, these oscillations are stabilized, causing more repeatable performance across cycles. This suggests that loads can serve as a damping mechanism, eliminating minor fluctuations. This is beneficial for cardiac assist applications, where sudden or erratic applications of excess force can trigger adverse effects. Improved stability also helps with sensor feedback and reduced noise.

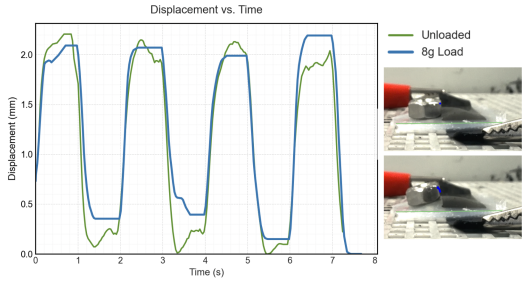

Fig. 5. **Displacement of HASEL actuator when loaded with an 8 gram mass, and compared to an unloaded HASEL.**

B. Sensor Performance

1) Calibration Curve: The integrated piezoresistive sensor was characterized by measuring the resistance as a function of the applied force. The sensor exhibited a nonlinear relationship between resistance and force, with resistance decreasing from 438 $k\Omega$ at 0 N of force to 90.5 $k\Omega$ at 0.16N. This is consistent with the increased contact area under load leading to reduced overall resistivity. The most sensitive range is observed to be between six and ten grams, or 0.078 N and 0.098 N, where the resistance sharply decreases even with small increases in force. Beyond this, the sensor's response begins to plateau again, suggesting saturation of the contact area.

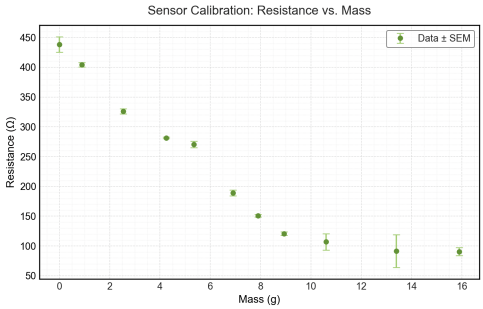

Fig. 6. Sensor calibration curve obtained by placing various masses on the sensor and recording resistance.

The most sensitive range is observed to be between six and ten grams, or 0.078 N and 0.098 N, where the resistance sharply decreases even with small increases in force. Beyond this, the sensor's response begins to plateau again, suggesting saturation of the contact area.

C. Coupled Performance

1) Time vs. Resistance: To assess the integration and real-time interaction of the actuator and sensor, we evaluated the system's response under varying applied voltages. Specifically, time-resolved resistance measurements were taken at voltages from 5 kV to 8 kV shown in Fig.7.

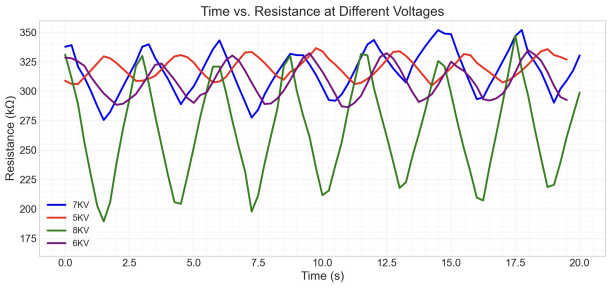

Fig. 7. Resistance of the sensor under the actuator's force output for multiple cycles at the following voltages: 5 kV, 6 kV, 7 kV, 8 kV.

The sensor exhibits a clear decrease in resistance with increasing voltage, reflecting the actuator's internal deformation and force output. At 5 kV, resistance decreases to 306.8 $k\Omega$. At 6 kV, the resistance decreases to 289.8 $k\Omega$. At 7kV, the resistance decreases to 285.6 $k\Omega$. At 8kV, the resistance decreases to 206.5 $k\Omega$. Figure 8 depicts these averages with respect to applied voltage. The sharp drop in resistance between 7 and 8 kV aligns with that found in Fig.6, where the sensitivity of the sensor is shown to increase. These responses indicate that the sensor can reliably detect actuation force through pressure feedback.

Additionally, the sensor demonstrates consistency across measurements. At different voltages, the sensor's resistance reports similar values across multiple actuation cycles, and

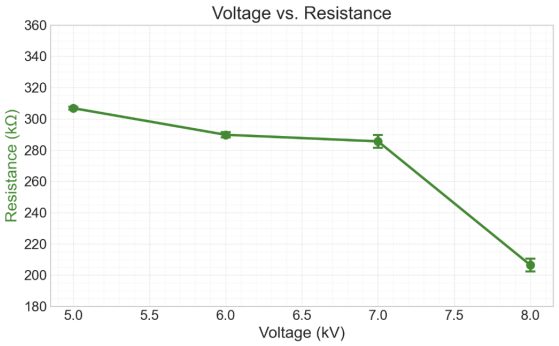

Fig. 8. Figure 8: Average minimum resistance as a function of applied voltage.

the baseline resistance during unloading does not deviate. This minimal hysteresis is made possible by the fluids present in the sensor, allowing it to reset after actuation. This is an important challenge to overcome in soft sensors, as hysteresis can lead to deviation of the readings and errors.

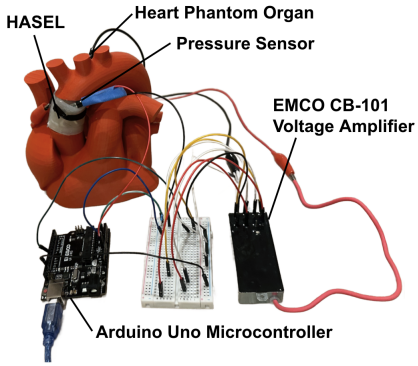

Fig. 9. Proposed closed-loop control of VAD.

The relationship between voltage, resistance, and force enables real-time feedback and control. As the voltage increases, the force exerted by the HASEL increases and is transmitted to the sensor. The changes in resistance can be correlated with a force output. Such properties support the implementation of closed-loop control, as shown in Figure 9, to maintain safe, consistent force delivery.

V. Conclusion

This work presents a fully 3D-printed HASEL integrated with a soft piezoresistive pressure sensor for cardiac assist applications. The actuator demonstrates deformation with sufficient strain and frequency for such applications. The sensor exhibits minimal hysteresis as a result of its fluidic reset characteristics, and when coupled with the actuator, is able to sense the force output of the device. These can be used to form a self-sensing system capable of real-time feedback without compromising the compliance of the device. It also enables closed-loop control, which will allow the actuator to adjust its output in response to its conditions and requirements. The integration of DIW 3D printing allows for customizable fabrication and improves reproducibility. The overall performance of the device supports its integration in cardiac assist devices for augmenting heart failure, as well as other biomedical applications. Future work will focus on in vivo testing to evaluate the system scenarios using phantom hearts.

References

[1] Cardiovascular diseases. (n.d.). World Health Organization. https://www.who.int/health-topics/cardiovascular-diseases#tab=tab_1. Retrieved January 12, 2025.

[2] J. Tu, L. Xu, F. Li, N. Dong, Developments and challenges in durable ventricular assist device technology: A comprehensive review with a focus on advancements in china, Journal of Cardiovascular Development and Disease, 11(1), 29. 2024.

[3] E. J. Molina, P. Shah, M. S. Kiernan, W. K. Cornwell, H. Copeland, K. Takeda, F. G. Fernandez, V. Badhwar, R. H. Habib, J. P. Jacobs, D. Koehl, J. K. Kirklin, F. D. Pagani, J. A. Cowger, The society of thoracic surgeons intermacs 2020 annual report, The Annals of Thoracic Surgery, 111(3), 2021, pp778-792.

[4] C. W. Tsao et al, Heart disease and stroke statistics—2023 update: A report from the american heart association, Circulation, 147(8), 2023.

[5] C. W. Yancy et al, 2013 accf/aha guideline for the management of heart failure. Journal of the American College of Cardiology, 62(16), e147-e239, 2013.

[6] A. P. Ambrosy et al, The global health and economic burden of Hospitalizations for heart failure. Journal of the American College of Cardiology, 63(12), 2014, pp1123-1133.

[7] S. A. Dual, J. Cowger, E. Roche, A. Nayak, The future of durable mechanical circulatory support: Emerging technological innovations and considerations to enable evolution of the field, Journal of Cardiac Failure, 30(4), 2024, pp596-609.

[8] I. Pirozzi, A. Kight, A. K. Han, M. R. Cutkosky, S. A Dual, Circulatory support: Artificial muscles for the future of cardiovascular assist devices, Advanced Materials, 36(43), 2023.

[9] L. G. Guex et al, Increased longevity and pumping performance of an injection molded soft total artificial heart. Soft Robotics, 8(5), 2021, pp588-593.

[10] E. T. Roche et al, Soft robotic sleeve supports heart function. Science Translational Medicine, 9(373), 2017.

[11] E. T. Roche et al, A bioinspired soft actuated material, Advanced Materials, 26(8), 2013, pp 1200-1206.

[12] K, M. Aarnink, F. R. Halfwerk, S. A. M. Said, J. G. Grandjean, J. M. J. Paulusse, Technical feasibility and design of a shape memory alloy support device to increase ejection fraction in patients with heart failure. Cardiovascular Engineering and Technology, 10(1), 2019 pp1-9.

[13] C. T. Starck, J. Becker, R. Fuhrer, S. Sundermann, J. W. Stark, V. Falk, Concept and first experimental results of a new ferromagnetic assist device for extra-aortic counterpulsation, Interactive CardioVascular and Thoracic Surgery, 18(1), 2013, pp13-16.

[14] T. Martinez et al, A novel soft cardiac assist device based on a dielectric elastomer augmented aorta: An in vivo study, Bioeng Transl Med, 8(2), 2023.

[15] M. Almanza et al, Feasibility of a dielectric elastomer augmented aorta. Advanced Science, 8(6), 2021.

[16] M. Duduta, E. Hajiesmaili, H. Zhao, R. J. Wood, D. R. Clarke, Realizing the potential of dielectric elastomer artificial muscles. Proceedings of the National Academy of Sciences, 116(7), 2019, pp2476-2481.

[17] M. Kellaris, V. Gopaluni Venkata, G. M. Smith, S. K. Mitchell, C. Keplinger, Peano-HASEL actuators: Muscle-mimetic, electrohydraulic transducers that linearly contract on activation. Science Robotics, 3(14), 2018.

[18] I. Pirozzi et al, Electrohydraulic vascular compression device (e-VaC) with integrated sensing and controls. Advanced Materials Technologies, 8(4), 2022.

[19] M. R. Vogt et al., High-Frequency Capacitive Sensing for Electrohydraulic Soft Actuators, 2024 IEEE/RSJ International Conference on Intelligent Robots and Systems (IROS), Abu Dhabi, United Arab Emirates, 2024, pp8299-8306.

[20] V. Sundaram et al., Embedded Magnetic Sensing for Feedback Control of Soft HASEL Actuators, IEEE Transactions on Robotics, vol. 39, no. 1, 2023, pp808-822.

[21] E. Luis, H. M. Pan, S. L. Sing, R. Bajpai, J. Song, W. Y. Yeong, 3D Direct Printing of Silicone Meniscus Implant Using a Novel Heat-Cured Extrusion-Based Printer. Polymers, 12(5), 2020, 1031.